PASSIVE SCALAR FLUX MEASUREMENTS IN THE NEAR-FIELD OF A SWIRLING JET

Ramis ÖRLÜ*, P. Henrik ALFREDSSON*

* Linné Flow Centre, KTH Mechanics, Osquars Backe 18, SE-100 44 Stockholm, Sweden

Summary The present experimental investigation is devoted to the heat flux characteristics of a passive scalar in the near-field region of a swirling jet issuing from a fully developed axially rotating pipe flow. A combined X-wire and cold-wire probe made it possible to access the instantaneous streamwise and azimuthal velocity components as well as the temperature simultaneously. Results indicate that the addition of swirl increases the integral scales and entrainment and thereby the streamwise passive scalar flux and shortens the distance and hence time needed to mix the jet with the ambient air.

1. INTRODUCTION

The addition of an azimuthal velocity component to a free turbulent round jet is widely known to entrain more ambient fluid [4], intensify the process of mass, momentum and heat transfer [1], spread and mix faster [3] and reduce noise production [13] and pollutant emission in the near-field of jet exhausts when compared to their non-swirling counterparts. All these features make swirling jets attractive for various technical applications. Despite the importance of this type of flows there are only few theoretical and numerical analysis that can be used in practical application. The limitations are due to the high Reynolds number required for Direct Numerical Simulations (DNS) [5], and due to the lack of reliable turbulence models for Reynolds Averaged Navier-Stokes equations (RANS) [8].

Although many experimental investigations have been initiated in the past 50 years (see review in [9]) there are discrepancies and contradicting results between them, making impossible any general conclusion. This is mainly due to the method by which the free jet, but especially the swirl, is generated. Stationary or rotating vanes, coil inserts, a rotating honeycomb, azimuthal injection of secondary flow upstream of the jet exit are just few examples of means to impart swirl to the flow. Hence there is a need for experiments with well-defined initial conditions in order to access the effect of rotation on the free round jet, both to provide direct information on the physics of these flows and to create a database that can be used to validate the numerical procedures and calibrate turbulence models.

The situation for the passive scalar, be it the concentration or temperature field, looks even more scarce. The experimental investigations known to the authors are mainly restricted to the far-field [3], to flow visualisations [12], the mean values [7], to swirling jets with recirculation zones [6] or those who are generated by means of passive vanes [1], which distort the flow regime near the outlet.

The present investigation aims to close this lack and hence focuses on the mixing characteristics and the passive scalar flux of a free swirling jet with swirl strength well below reverse flow on the central axis, whereby the jet, emanating from a fully developed axially rotating pipe flow, is slightly heated in order to facilitate the temperature as a passive scalar. By utilising a fully developed pipe flow it was ensured that no secondary flows or traces of

swirl generating methods are produced and furthermore well-defined initial conditions for the jet were provided.

Simultaneous measurements of the streamwise and azimuthal velocity component as well as the temperature performed by means of a combined X-wire and cold-wire probe enabled the study of the dynamic and thermal (passive scalar) field in a swirling jet flow free from any traces and asymmetries in the radial distributions, due to the swirl generating mechanisms. Thereby the observed alterations in the well-defined dynamically and thermally axisymmetric flow field could solely be ascribed to the effect of swirl, which in our view is an unique contribution in regards to the passive scalar field in swirling jet flows.
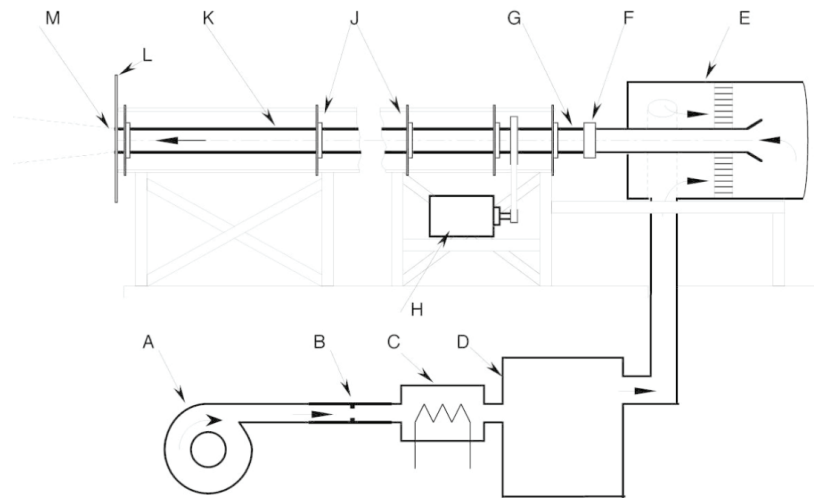
Fig. 1. Schematic of the experimental setup. A) Centrifugal fan. B) Flow meter, C) Electrical heater, D) Distribution chamber, E) Stagnation chamber, F) Coupling between stationary and rotating pipe, G) Honeycomb, H) DC motor, J) Ball bearings, K) Rotating pipe, L) Circular end plate, M) Pipe outlet

2. EXPERIMENTAL SETUP AND PARAMETERS

2.1. Experimental facility

The experiments are performed at the *Fluid Physics Laboratory* of *KTH Mechanics* in a specially designed setup, consisting of a 100 pipe diameters long axially rotating pipe as shown in Fig. 1, which was recently used to study the dynamics of swirling flows in the near-field region [2]. The air is provided by a centrifugal fan (A), downstream of which a flow meter (B) monitors the flow rate. After the flow meter a flow distribution chamber (D) distributes the flow into three different pipes, which are symmetrically fed into the stagnation chamber (E). A bell mouth shaped entrance first feeds it into a one meter long stationary section, which is connected to the rotating pipe (K) through a rotating coupling (F). In the first part of the rotating part of the pipe a honeycomb (G) is mounted, which brings the flow into more or less solid body rotation. Thereafter the flow develops along the 6 meter long pipe before it emanates as a free jet (M). The pipe is made of seamless steel and has a honed inner surface. It is supported along its full length by 5 roller bearings (J), which are mounted within a rigid triangular shaped framework, and it is belt driven via a feed back controlled DC motor (H). In the present measurements the pipe ends with a 30 cm diameter circular end plate (L). A heater (C) placed in the flow upstream of the distribution chamber provides the heating of the air. The heater power

can be regulated and is typically around 800 W. The outer pipe surface is insulated with a 15 mm foam material in order to establish a constant radial temperature. The typical temperature difference between the flow in the pipe and the ambient air is 12 K.
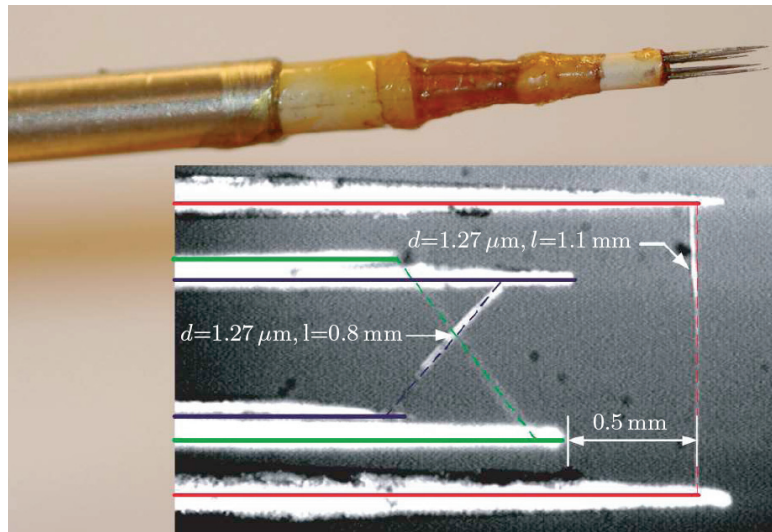
Fig. 2. Combined X-wire and cold-wire probe with close-up of probe and wire constellation. All wires are soldered to the tip of the prongs, which is not apparent from the two-dimensional microscopic picture.

2.2. Measurement technique

In order to get simultaneous acquisition of velocity and temperature, a specific home made probe has been designed and built, which consists of a combined X-wire and cold-wire probe operated in constant temperature (CTA) and constant current (CCA) mode, respectively. The cold-wire consists of an 1.1 mm long wire and is placed 0.5 mm upstream and parallel between the 0.8 mm long hot-wires forming the X-probe in order to minimise the thermal and wake interference. All sensing elements are Platinum wires with a diameter of 1.27 micron. In order to extend the applicability of the combined probe as much as possible into the intermittent region the resistance overheat ratio of the hot-wires and the current through the cold-wire were reduced to 30 % and 0.3 mA, respectively. The X-probe was calibrated in the potential core of a specially designed contraction jet facility for different velocities and yaw angles at a constant temperature according to the look-up inversion method, whereas the cold-wire was calibrated in the centre of the pipe exit against thermocouples with a measurement resolution of 0.1 K. Due to the small diameter and the low current through the cold-wire the anemometer output becomes a linear function of the fluid temperature and practically insensitive to velocity changes in the range of interest. While the instantaneous temperature can be measured directly by the cold-wire, the voltage output for the hot-wires have been compensated for changes in the instantaneous fluid temperature. Further details on the measurement technique as well as an assessment of the reliability of the results in the highly intermittent region can be found in [9].

The signals from the CTA and CCA channels of an AN-1003 hot-wire anemometry system were offset and amplified through the circuits to match the fluctuating signal components to the voltage range of the 16-bit A/D converter used, and then digitised on a PC at a sampling frequency of 4 kHz and a sampling duration between 30 s and 60 s depending on the downstream position of the probe.

2.3. Experimental parameters

The flow in a fully developed axially rotating pipe flow is commonly characterised by its Reynolds number

$$\text{Re}_D = 2U_b R/\nu \,, \tag{3}$$

and swirl number

$$S = V_w/U_b \,, \tag{4}$$

where U_b is the bulk velocity, R the pipe radius, ν the kinematic viscosity and V_w the azimuthal velocity of the rotating pipe. For swirling jets, with different swirl generating methods it is more convenient to utilise an integral swirl number defined as the ratio between the angular momentum to the axial momentum times the radius,

$$S_{\phi x} = \frac{\int_0^\infty r^2 UV\, dr}{R \int_0^\infty r\,(U^2 - V^2)\, dr} \,, \tag{5}$$

where U and V denote the mean axial and azimuthal velocity component as depicted in Fig. 3. However different flow fields can be observed for the same Re_D and $S_{\phi x}$, making it absolutely essential to provide well defined initial conditions to classify the results, which, by the fully developed axially rotating pipe flow, is per se fulfilled.

The present experiments were conducted at a Reynolds number of about 24000 and an excess temperature (above ambient temperature) of about 12 K for both non-swirling and swirling jets. The swirl number for the swirling jet was fixed at 0.5, which corresponds to an integral swirl number of approximately 0.15, well below the occurrence of vortex breakdown. Full radial profiles of the axial and azimuthal velocity as well as temperature were acquired starting from the pipe outlet with an increment of one diameter up to $x/D = 6$.
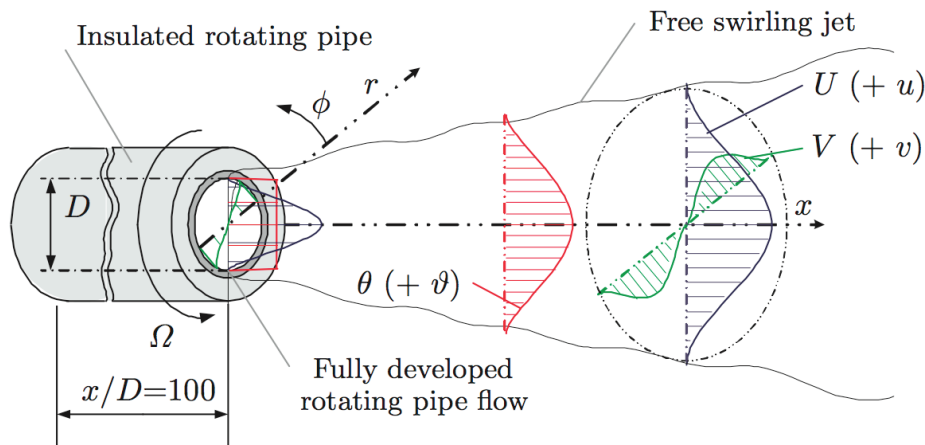
Fig. 3. Schematic of the cylindrical coordinate system of the free developing heated swirling jet emanating from a fully developed axially rotating pipe flow.

535

3.   RESULTS AND DISCUSSION

3.1.   Mean flow development

Three-dimensional profiles of the mean axial velocity component and mean temperature are visualised in Fig. 3, thus making it possible to follow the evolution of the mean quantities along their radial and axial directions at the same time. The time-averaged values were normalised using the bulk velocity, U_b, and the centreline mean temperature (relative to ambient) at the pipe outlet of the non-swirled jet, θ_0, in order to emphasise the effect of the rotation on both the flow dynamics as well as the passive contaminant. Thick dashed lines are drawn through the centreline values (U_{CL}^* and θ_{CL}^*) as well as through the half-widths (R_U and R_θ) of the streamwise velocity component and temperature, representing the position where the considered quantity reaches half the value of its centreline value. The former depicts the axial decay rate and is often used as an indicator for mixedness while the latter facilitates the presentation of the spreading of the jet and hence visualises the entrainment rates for both the momentum (black lines) and heat (grey lines), respectively.

A recognisable feature of the thermal field is that its centreline value remains almost constant for downstream positions up to four pipe diameters, whereas the centreline streamwise velocity component decreases (weakly) continuously right from the beginning of the pipe outlet. Therefore one could define a thermal potential core extending to four pipe diameters, whereas no dynamic potential core exists by definition. The different boundary conditions for the temperature and velocity can be used to explain this behaviour. It is clearly recognisable that the addition of swirl increases the mean streamwise velocity as well as the mean temperature for the first diameters downstream of the pipe outlet while in regions beyond three and four diameters downstream the axial velocity component and temperature are overtaken by the non-swirling centreline values, thus indicating the faster axial decay rates through the addition of swirl. Due to the absence of source and sink terms in the governing equations for the passive scalar the increase in the temperature at the pipe outlet for the swirling jet has to be brought about by the dynamic field. Reynolds analogy can be utilised to link the increase in temperature in a wide central region to the increase of the streamwise velocity component.

3.2.   Turbulence development

The turbulence intensities summarised in the three-dimensional profiles in Fig. 4 provide another possibility to analyse the mixing behaviour in the near-field of the jet. As evident from the off-axis peaks and the strong valleys around the centreline for all measured fluctuating components the heated jet fluid is not well mixed with the entrained cold air. However with increasing downstream position the valley looses its extreme difference to the maximum value indicating the transition towards the well mixed and developed jet. The addition of swirl clearly enhances the centreline values (dashed lines) for all turbulence intensities starting from 2-3 pipe diameters having their largest difference to the non-swirled jet at 4-5 exit diameters. This confirms the global effect of swirl to enhance mixing. The axial decays of the non-swirling (grey dashed lines) and swirling (black dashed line) jet visualises this enhancement through their parted trends which seem to converge further downstream due to the restriction of full mixedness.

Although there is no dynamic potential core in the present case the free shear flow emanating from the pipe exit maintains its low turbulence intensity along and around the

centreline until the strong conical shear layer initiating from the pipe edge reaches the centreline. From there on all root mean square values of the velocity and temperature fluctuations are increasing rapidly. The increased entrainment, due to the addition of swirl, shortens the distance for the strong conical shear layer to reach the centreline and hence shortens the distance needed for transition from fully developed turbulent pipe flow to developing jet flow.
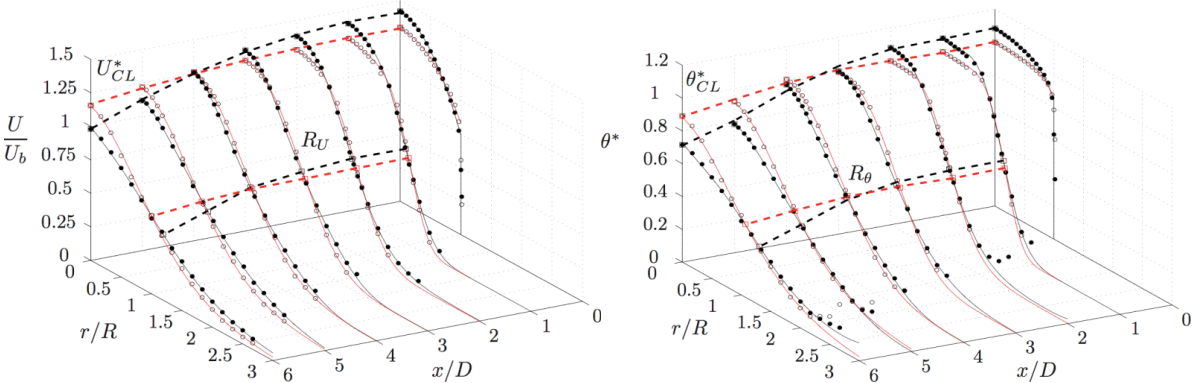
Fig. 4. Three-dimensional profiles of the non-dimensionalised mean axial velocity (left figure) and temperature (right figure) for the non-swirled (open markers) and swirled (filled markers) jet. Axial decays (U_{CL}^* and θ_{CL}^*) and mean velocity and temperature half-widths (R_U and R_θ) are illustrated through the dashed lines. Black lines in the radial direction correspond to the jet with swirl, while grey lines visualise the quantities for the non-swirling jet. Full lines are for visual aid only.
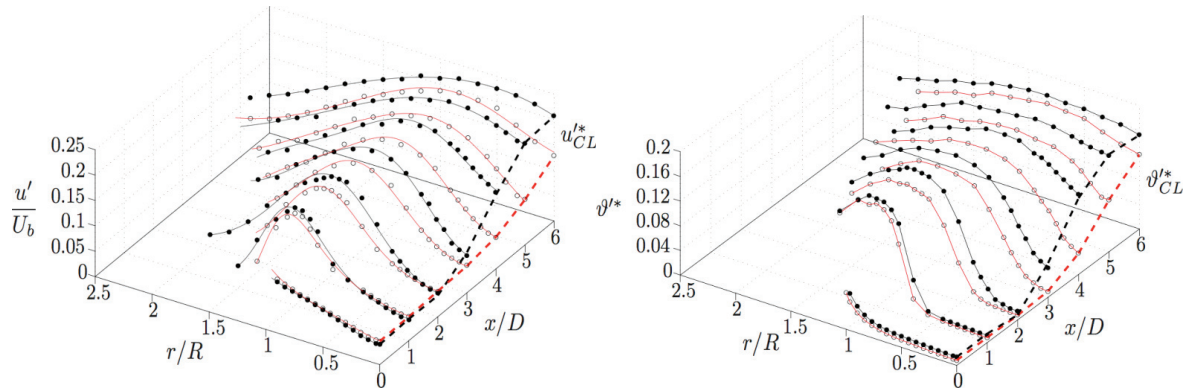
Fig. 5. Three-dimensional profiles of the non-dimensionalised root mean square value of the axial velocity (left figure) and temperature (right figure) fluctuations for the non-swirled (open markers) and swirled (filled markers) jet. Their centreline developments (u_{CL}' and ϑ_{CL}') are illustrated through the dashed lines. Full lines are for visual aid only.

3.3.   Streamwise passive scalar flux

The correlation coefficient of axial velocity and temperature fluctuations, $\rho_{u\vartheta}$, as well as the streamwise passive scalar flux, $\overline{u\vartheta}^* = \overline{u\vartheta}/U_b\theta_0$, across the heated jet are visualised for different downstream positions in Fig. 5. No differences are detectable between the non-swirling and swirling jet for the fully developed pipe flow as well as the farthest measured downstream position, while only marginal differences are observable at $x/D = 2$. In contrast, a distinct difference can be found four pipe diameters downstream, where the addition of swirl increases the correlation between the instantaneous axial velocity component and the temperature remarkably, which could be anticipated through the increase of the root mean square value of both fluctuating variables as shown in Fig. 4. Clearly a change in the turbulence structure has occurred keeping in mind that the mean axial velocity component and temperature at this downstream position is rather unchanged as evident from Fig. 3. Hence swirl strongly promotes the longitudinal turbulent heat flux in a central region of the jet between $3 \leq x/D \leq 5$.

The low values of the correlation coefficient of axial velocity and temperature fluctuations, as e. g. observed around the centreline at 4 pipe diameters downstream in the case of the non-swirling jet, are an indication for the unmixedness of the flow at that particular local position and are a result of the thermal potential core. As evident from higher statistical moments these regions correspond to highly thermal intermittent regions, meaning that cold air 'blobs' are probably reaching or crossing the centreline of the warm air stream. The addition of rotation shortens the thermal cone and causes a drastic increase in the streamwise heat flux, especially 3-5 diameters downstream along and around the centreline, and remains also over the whole cross-section larger than its non-swirling counterpart.
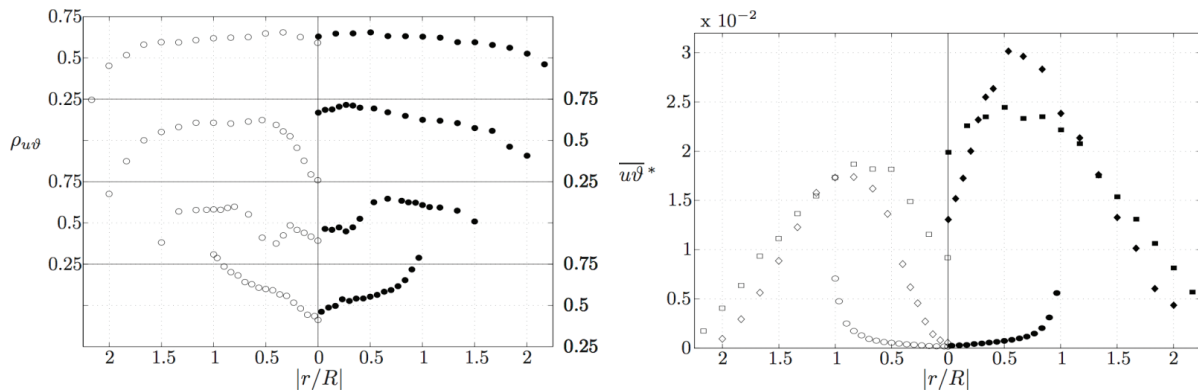
Fig. 6. Correlation coefficient of axial velocity and temperature fluctuations (left figure) and streamwise passive scalar flux (right figure) across the heated non-swirled (open symbols) and swirled (filled symbols) jet from bottom to top corresponding to $x/D =$ 0, 2, 4 and 6 (left figure) and ○: $x/D = 0$, ◇: $x/D = 4$, □: $x/D = 6$ (right figure).

3.4.   Spectral analysis

To illustrate the difference in the turbulence structure of the flow due to the addition of rotation the spectral content, the power spectral density scaled by the square of the bulk velocity, is presented across the heated non-swirled and swirled jet at a downstream position of $4D$ in Fig. 6.

In the case of the non-swirling jet a distinct peak ($f = 55\,Hz$) can be seen along the centreline, whereas in the case of the swirling jet a broader peak, shifted towards lower frequencies and hence larger length scales, can be observed along with a generally higher energy level. This is connected to the previously mentioned conical shear layer surrounding the low turbulence intensity region, which due to the addition of swirl reached the centreline earlier and gives rise to the increased heat flux.
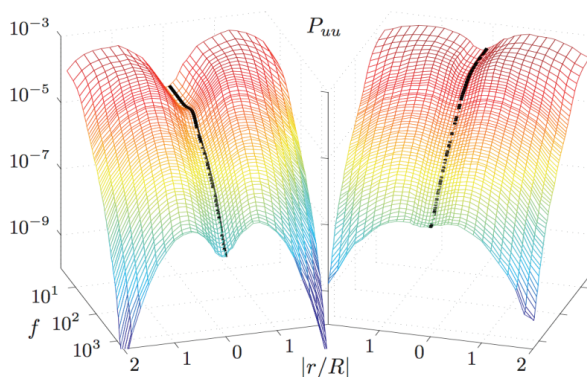
Fig. 7. Power spectral density of the streamwise velocity fluctuations across the jet for the non-swirled (left figure) and swirled jet (right figures) at $x / D = 4$.

4.   CONCLUSION

It was shown possible to use a combined X-wire and cold-wire probe to measure the axial and azimuthal velocity components as well as the temperature simultaneously and by this the turbulent fluxes of heat in the axial direction as well as their correlation.

The addition of a moderate degree of swirl highly modifies the dynamic and thermal flow field of the jet in its near-field region to that effect that the swirling jet in comparison to its non-swirling counterpart spreads and mixes faster as well as increases momentum and heat transfer rates. Whereas no significant change in the turbulence structure is detectable within the first two pipe diameters, a considerable change around four pipe diameters downstream is found, which shortens the downstream distance and hence time needed to mix the jet with the ambient air.

Connected to this the integral time and hence length scale of the turbulence is found to increase with the addition of swirl indicating that an increase of the integral scale is related to faster mixing.

The present study showed that hot-wire anemometry can be applied in complex flows with high local turbulence intensity and intermittency, three-dimensionality in the mean velocity as well as non-isothermal conditions, which are all known to restrict the applicability of hot-wire anemometry. Furthermore it was possible to extract information about velocity and temperature correlations as well as the spectral content of the flow in a wide central region, with the limitations in mind, which by other means could not be accessed in such quality.

ACKNOWLEDGEMENT

REFERENCES

[1]   Elsner, J.W., Kurzak, L.: Characteristics of turbulent flow in slightly heated free swirling jets. J. Fluid Mech. 180, 147–160 (1987)

[2]   Facciolo, L., Tillmark, N., Talamelli, A., Alfredsson, P.H.: A study of swirling turbulent pipe and jet flows. Physics of Fluids 19(3), 035105 (2007)

[3]   Grandmaison, E.W., Becker, H.A.: Turbulent mixing in free swirling jets. Can. J. Chem. Eng. 60, 76–82 (1982)

[4]   Gupta, A.K., Lilley, D.G., Syred, N.: Swirl flows. ABACUS Press, Cambridge, USA (1985)

[5]   Hu, G.H.; Sun, D.J. & Yin, X.Y.: A numerical study of dynamics of a temporally evolving swirling jet. Phys. Fluids 13, 951-965 (2006)

[6]   Komori, S., Ueda, H.: Turbulent flow structure in the near field of a swirling round free jet. Phys. Fluids 28, 2075–2082 (1985)

[7]   Kuroda, C., Ogawa, K., Inoue, I.: Mixing in swirling jet. J. Chem. Eng. Jpn. 18, 439–445 (1985)

[8]   Morse, A. P.: Axisymmetric Turbulent Shear Flows with and without Swirl. Ph.D. Thesis, University of London, UK (1980)

[9]   Örlü, R.: Experimental study of passive scalar mixing in swirling jet flows. TeknL thesis, KTH Mechanics, Stockholm, Sweden (2006). TRITA-MEK Tech. Rep. 2006:11

[10] Rose, W.G.: A swirling round turbulent jet; 1 - Mean-flow measurements. J. Appl. Mech. 29, 615–625 (1962)

[11] Sislian, J.P., Cusworth, R.A.: Measurements of mean velocity and turbulent intensities in a free isothermal swirling jet. AIAA J. 24, 303–309 (1986)

[12] Toh, I.K., Honnery, D., Soria, J.: Velocity and scalar measurements of a low swirl jet. In: Proc. 4th Australian Conf. Laser Diagnostics Fluid Mech. Comb., pp. 129–132. The University of Adelaide, South Australia, Australia (2005)

[13] Wooten, D.C., Wooldridge, C.E., Amaro, A.J.: The structure of jet turbulence producing jet noise. Tech. rep., Stanford Research Institute, California, USA (1972). SRI Project 8139